British Journal of Pharmacology

British Journal of Pharmacology (2018) **175** 2284–2295 2284

Themed Section: Recent Advances in Targeting Ion Channels to Treat Chronic Pain

RESEARCH PAPER

Inhibition of human N- and T-type calcium channels by an *ortho*-phenoxyanilide derivative, MONIRO-1

Correspondence David J Adams, Illawarra Health and Medical Research Institute (IHMRI), University of Wollongong, Wollongong, NSW 2522, Australia. E-mail: djadams@uow.edu.au

Received 14 December 2016; **Revised** 24 March 2017; **Accepted** 5 June 2017

Jeffrey R McArthur[1,2], Leonid Motin[1,2], Ellen C Gleeson[3,4], Sandro Spiller[4], Richard J Lewis[5], Peter J Duggan[3,6], Kellie L Tuck[4] and David J Adams[1,2]

[1]Illawarra Health and Medical Research Institute, University of Wollongong, Wollongong, NSW, Australia, [2]Health Innovations Research Institute, RMIT University, Melbourne, VIC, Australia, [3]CSIRO Manufacturing, Bag 10, Clayton South, VIC, Australia, [4]School of Chemistry, Monash University, Clayton, VIC, Australia, [5]Institute for Molecular Bioscience, The University of Queensland, St Lucia, QLD, Australia, and [6]School of Chemical and Physical Sciences, Flinders University, Adelaide, SA, Australia

BACKGROUND AND PURPOSE

Voltage-gated calcium channels are involved in nociception in the CNS and in the periphery. N-type ($Ca_v2.2$) and T-type ($Ca_v3.1$, $Ca_v3.2$ and $Ca_v3.3$) voltage-gated calcium channels are particularly important in studying and treating pain and epilepsy.

EXPERIMENTAL APPROACH

In this study, whole-cell patch clamp electrophysiology was used to assess the potency and mechanism of action of a novel *ortho*-phenoxylanilide derivative, MONIRO-1, against a panel of voltage-gated calcium channels including $Ca_v1.2$, $Ca_v1.3$, $Ca_v2.1$, $Ca_v2.2$, $Ca_v2.3$, $Ca_v3.1$, $Ca_v3.2$ and $Ca_v3.3$.

KEY RESULTS

MONIRO-1 was 5- to 20-fold more potent at inhibiting human T-type calcium channels, $hCa_v3.1$, $hCa_v3.2$ and $hCa_v3.3$ (IC_{50}: 3.3 ± 0.3, 1.7 ± 0.1 and 7.2 ± 0.3 μM, respectively) than N-type calcium channel, $hCa_v2.2$ (IC_{50}: 34.0 ± 3.6 μM). It interacted with L-type calcium channels $Ca_v1.2$ and $Ca_v1.3$ with significantly lower potency ($IC_{50} > 100$ μM) and did not inhibit $hCa_v2.1$ or $hCa_v2.3$ channels at concentrations as high as 100 μM. State- and use-dependent inhibition of $hCa_v2.2$ channels was observed, whereas stronger inhibition occurred at high stimulation frequencies for $hCa_v3.1$ channels suggesting a different mode of action between these two channels.

CONCLUSIONS AND IMPLICATIONS

Selectivity, potency, reversibility and multi-modal effects distinguish MONIRO-1 from other low MW inhibitors acting on Ca_v channels involved in pain and/or epilepsy pathways. High-frequency firing increased the affinity for MONIRO-1 for both $hCa_v2.2$ and $hCa_v3.1$ channels. Such Ca_v channel modulators have potential clinical use in the treatment of epilepsies, neuropathic pain and other nociceptive pathophysiologies.

LINKED ARTICLES

This article is part of a themed section on Recent Advances in Targeting Ion Channels to Treat Chronic Pain. To view the other articles in this section visit http://onlinelibrary.wiley.com/doi/10.1111/bph.v175.12/issuetoc

Abbreviations

hERG, human ether à-go-go related gene; SSI, steady-state inactivation; VGCCs, voltage-gated calcium channels

DOI:10.1111/bph.13910

Introduction

Sensory nerve conduction relies on the coordinated activation of a suite of ion channels to generate fast and accurate responses to mechanical, thermal and chemical stimuli. In the periphery, harmful signals are perceived by 'nociceptive' neurons and relayed centrally *via* voltage-activated ion channels (**K_v**, **Na_v**, **Ca_v**) and ligand-gated ion channels (**TRP**, **K_{2P}**, **P2X**) (Waxman and Zamponi, 2014) as part of the 'pain-signalling cascade' (Gold and Gebhart, 2010). In chronic pain, these pathways are characterized by hyperactivity (Waxman and Zamponi, 2014), and the effects of noxious stimuli are enhanced (hyperalgesia) to the point where non-noxious stimuli are painful (allodynia) (see Guo and Hu, 2014). Voltage-gated calcium channels (VGCCs) involved in pain pathways are localized to dendrites of primary sensory neurons and contribute to integrate nociceptive stimuli at the spine by regulating the release of pro-nociceptive neurotransmitters, including substance P, calcitonin gene-related peptide and glutamate, at the presynaptic nerve terminus (Simms and Zamponi, 2014). Therefore, modulating specific Ca_v subtypes could be a promising way to treat chronic pain.

Five distinct voltage-gated calcium current types have been described in mammalian cells: L- (**$Ca_v1.1$**, **1.2**, **1.3** and **1.4**), P/Q- (**$Ca_v2.1$**), N- (**$Ca_v2.2$**), R- (**$Ca_v2.3$**) and T- (**$Ca_v3.1$**, **3.2**, **3.3**) types (Catterall *et al.,* 2005). Importantly, each Ca_v subtype has distinct electrophysiological properties, tissue-specific localization and pharmacological profiles (Catterall *et al.,* 2005). N-type calcium channels have been a major focus of research because they are localized at the presynaptic terminals of sensory nerves in the dorsal horn of the spinal cord, where they play a critical role in pain signalling (Saegusa *et al.,* 2001; Lee, 2014). As a result, $Ca_v2.2$ channels are strongly implicated in a range of chronic pain conditions including neuropathic pain (pain caused by injury to the nervous system). Specific $Ca_v2.2$ channel inhibitors have clinical applications (Altier and Zamponi, 2004; Perret and Luo, 2009; Bourinet *et al.,* 2014), such as **ω-conotoxin MVIIA** (Ziconotide). Ziconotide selectively targets $Ca_v2.2$ channels and is used to effectively treat intractable chronic pain conditions (Pope and Deer, 2013). However, due to its chemical nature, Ziconotide must be administered into the cerebrospinal fluid *via* the intrathecal route and has a relatively narrow therapeutic window (Pope and Deer, 2013).

T-type calcium channels modulate neuronal excitability in the peripheral and central nervous systems, where they are linked to hyperexcitable states such as epilepsy, pain and tremor disorders like Parkinson's disease (Bourinet *et al.,* 2005; Choi *et al.,* 2007; Kim *et al.,* 2001). Previously characterized T-type calcium channels inhibitors, such as mibefradil and ethoximide, have analgesic properties, suggesting that T-type channels may be involved in pain signalling (Matthews and Dickenson, 2001; Todorovic *et al.,* 2002; Flatters and Bennett, 2004; Wen *et al.,* 2010). Unfortunately, **mibefradil** and ethoximide target a wide range of voltage-gated ion channels, including sodium, potassium and chloride channels (Chouabe *et al.,* 1998; Nilius *et al.,* 1998; Eller *et al.,* 2000).

To overcome this lack of specificity, small molecule T-type calcium channel inhibitors were designed and have been shown to provide analgesic effects in mouse models of inflammatory and neuropathic pain (Kraus *et al.,* 2010; Reger *et al.,* 2011; Bladen *et al.,* 2015). Of particular note is the analgesic, low MW compound **TTA-A2**, which is more potent against inactivated than closed or resting channels (IC_{50} values of 100 and 10 μM at $Ca_v3.1$ respectively), indicating its effects on targets are state-dependent (Francois *et al.,* 2013). Based on these findings, N- and T-type calcium channels are of particular interest for the study and treatment of chronic pain (see recent reviews by Cheong and Shin, 2013; Lee, 2013; Sekiguchi and Kawabata, 2013; François *et al.,* 2014; Lee, 2014; Simms and Zamponi, 2014).

During the last 5 years, numerous reports have described small molecule $Ca_v2.2$ channel inhibitors as alternatives to Ziconotide (see review by Lee, 2014). Regrettably, clinical development of the most promising of these small-molecules, Z160, a reformulated form of **NP118809** (Zamponi *et al.,* 2009) (compound **1**, Figure 1), was discontinued after it failed to meet end points in phase II clinical trials (Eller *et al.,* 2000). Due to this and the need for effective and safe therapeutics for chronic pain, the development of new classes of small-molecule Ca_v channel antagonists is of significant interest.

The pharmacophore of $Ca_v2.2$-selective **ω-conotoxin GVIA** (McCleskey *et al.,* 1987; Baell *et al.,* 2004; Baell *et al.,* 2006; Andersson *et al.,* 2009; Duggan *et al.,* 2009) has been carefully studied and has led to the identification of a series

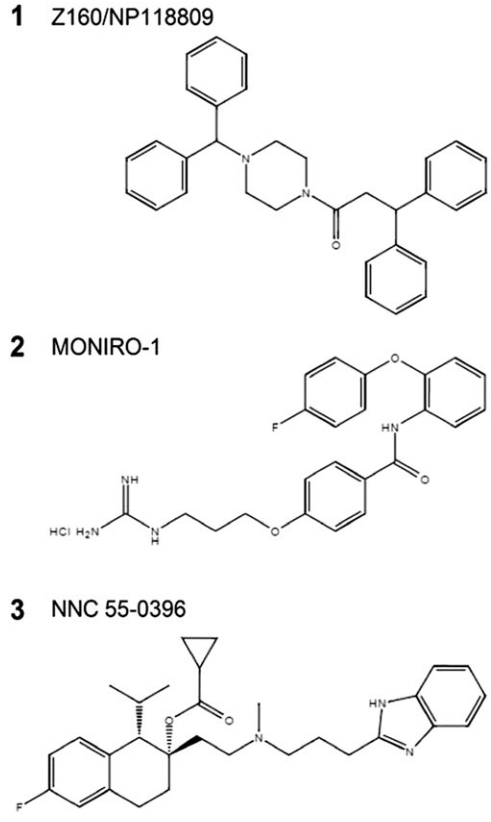

Figure 1

Chemical structures of compounds **1** (Z160/NP118809), **2** (MONIRO-1) and **3** (NNC 55-0396) relevant to this study.

of compounds that block $Ca_v2.2$ channels in a concentration-dependent manner (Tranberg *et al.,* 2012).

We focused on developing low MW calcium channel inhibitors with enhanced biophysical properties including reversibility, voltage- and/or state-dependence. Compounds acting *via* these mechanisms can strongly inhibit channels upon membrane depolarization (Hondeghem and Katzung, 1984; Butterworth and Strichartz, 1990) by preferentially targeting the open and/or inactivated states over the resting state. Such compounds would facilitate inhibition of high-frequency firing or depolarised nerves that can predominate in chronic pain states and could act within a wider therapeutic window.

To develop these calcium channel inhibitors, we screened a small library of related derivatives, using FLIPR Tetra® high-throughput cellular screening system, for their ability to inhibit $Ca_v2.2$-mediated calcium responses in SH-SY5Y cells using the fluorescent indicator Calcium 4 dye (Molecular Devices, Sunnyvale, CA, USA) (Gleeson *et al.,* 2015). In this assay, MONIRO-1 (compound **2**, Figure 1) inhibited Ca^{2+} responses elicited by KCl-mediated depolarization with an IC_{50} of 124 μM. Subsequently, we characterized the *ortho*-phenoxyanilide derivative MONIRO-1 electrophysiologically. To directly assess the biophysical properties of MONIRO-1 inhibition of VGCCs, we used the whole-cell patch clamp recording technique to study a comprehensive array of Ca_v channels heterologously or stably expressed in HEK-293 cells. MONIRO-1 was 5–100 times more potent against T-type calcium channels ($Ca_v3.1$, $Ca_v3.2$ and $Ca_v3.3$) than N-type ($Ca_v2.2$) and L-type ($Ca_v1.2$ and $Ca_v1.3$) channels. No inhibition of P/Q ($Ca_v2.1$) or R-type currents ($Ca_v2.3$) was detected in the presence of up to 100 μM MONIRO-1. Furthermore, MONIRO-1 modulated $Ca_v2.2$ differently at various stimulation rates and in a state-dependent fashion, preferentially inhibiting hyperactive channels such as those likely to predominate in pathologically augmented pain states.

Methods

Cell culture and transfection

HEK293 cells containing the SV40 Large T-antigen (HEK293T) were cultured at 37°C, 5% CO_2 in Dulbecco's Modified Eagle's Medium (Invitrogen Life Technologies, Australia) supplemented with 10% fetal bovine serum (Invitrogen), 1% penicillin and streptomycin (Invitrogen). HEK293T cells stably expressing the human $Ca_v2.1$ (P/Q-type) calcium channel (α_{1A-2} splice variant; GenBank accession no. AF004883.1), $Ca_v2.2$ (N-type) calcium channel (transcript variant 1, NM_000718) or $Ca_v2.3$ (R-type) calcium channel (neuronal α_{1E-3} splice variant, also called α_{1E-c}, L29385.1) were obtained from Merck and cultured according to procedures described by Dai *et al.* (2008). These cell lines co-express recombinant human Ca_v $\alpha_{2b}\delta$-1 (M76559.1) and Ca_v β_{3a} (NM_000725) auxiliary subunits (Dai *et al.,* 2008). Cells are plated onto 12 mm cover glass and incubated at 30°C, 5% CO_2 for 24–48 h prior to recording.

In a separate series of experiments, HEK293T cells were transiently co-transfected with plasmid cDNAs encoding mouse $Ca_v1.2$ (provided by Dr D. Lipscombe, Addgene plasmid # 26572; Helton *et al.*, 2005) or human $Ca_v1.3$ (provided by Dr G. Zamponi, University of Calgary) with $\alpha_2\delta$-1 and β_3, $Ca_v3.1$ (provided by Dr G. Zamponi), human $Ca_v3.2$ (CACNA1HB; Origene Technologies, Rockville, MD), human $Ca_v3.3$ a1Ic-HE3-pcDNA3 was a gift from Dr E. Perez-Reyes (Gomora *et al.,* 2002) (Addgene plasmid # 45810) and $K_v11.1$ (human ether à-go-go related gene [hERG]) (provided by Dr J. Vandenberg, Victor Chang Cardiac Research Institute, Sydney). After transfection, cells were plated on glass coverslips and incubated at 37°C, 5% CO_2 overnight. The transfection medium was then replaced with culture medium, and cells were incubated at 30°C, 5% CO_2.

Electrophysiology

Electrophysiological experiments were carried out 1–3 days after transfection using the whole-cell patch clamp recording technique. Cells were superfused with a solution containing 110 mM NaCl, 10 mM $CaCl_2$, 1 mM $MgCl_2$, 5 mM CsCl, 30 mM TEA-Cl, 10 mM D-glucose and 10 mM HEPES, pH 7.4 with TEA-OH (~310 mOsmol kg^{-1}). Fire-polished borosilicate patch pipettes with tip-resistance values of 1–3 MΩ were filled with an intracellular solution containing 125 mM K^+gluconate, 5 mM NaCl, 2 mM $MgCl_2$, 5 mM EGTA, 4 mM MgATP and 10 mM HEPES, pH 7.2 with CsOH (~300 mOsmol kg^{-1}). Depolarization-activated calcium currents were recorded at room temperature (21–23°C) using a Multiclamp 700B patch clamp amplifier (Molecular Devices, Sunnyvale, CA, USA) controlled by Digidata 1322A/Clampex 9.2 acquisition systems. MONIRO-1 stock solution was dissolved in 5% DMSO to a concentration of 5 mM. MONIRO-1 was further diluted in recording solution to appropriate concentrations. Previous experiments using the maximal concentration of DMSO used, 0.1% at 100 μM, did not modulate VGCC currents in recording solution.

Depolarization-activated calcium currents (I_{Ca}) were evoked from a holding potential of −80 mV, with a 135 ms (50 ms for T-type) voltage step to a test potential (determined from peak of I-V curve) applied every 10 s. When evaluating I_{Ca} amplitude in the presence and absence of various compounds, test depolarizations of varying durations were applied at a frequency of 0.03–2 Hz, from a holding potential of −60, −80 or −100 mV to a test potential determined from an I–V relationship to elicit peak inward current. To examine the effects of pulse duration on MONIRO-1 block and recovery from block, pulses of either 45 or 135 ms for $Ca_v2.2$ (30 μM) or 15 or 50 ms for $Ca_v3.1$ (3 μM) were elicited at a frequency of 0.1 Hz (V_h = −80 mV). Similarly, to study the frequency dependence of MONIRO-1 inhibition, test pulses (45 ms for $Ca_v2.2$ or 15 ms for $Ca_v3.1$) were elicited at rates of 0.03, 0.1 and 0.2 Hz for $Ca_v2.2$ (10 μM MONIRO-1) and 0.03, 0.1, 0.2, 1 and 2 Hz for $Ca_v3.1$ (3 μM MONIRO-1). To determine the time constants for activation and inactivation of macroscopic currents, we used a single exponential equation to fit the traces in control and after MONIRO-1 application.

Activation curves were measured from test pulses from −80 to +80 mV every 5 mV for $Ca_v2.2$ and $Ca_v3.1$ channels (V_h = −80 mV) before and after MONIRO-1 application. Steady-state inactivation (SSI) curves were generated from various pre-pulse potentials (−120 to 0 mV for $Ca_v2.2$; −85 to −20 mV for $Ca_v3.1$) of 10 s ($Ca_v2.2$) or 1 s ($Ca_v3.1$).

Recovery from inactivation was examined using a double-pulse protocol, varying the time between a fully inactivating pre-pulse and the test pulse repeated every 15 s, using a concentration of MONIRO-1, which inhibits ~50% of the current. Recovery data were best fit by a double exponential. Currents were filtered at 3 kHz and sampled at 10 kHz. Leak and capacitive currents were subtracted using a −P/4 pulse protocol. Data were stored digitally on a computer for further analysis.

Data analysis

The data and statistical analysis comply with the recommendations on experimental design and analysis in pharmacology (Curtis *et al.*, 2015). All data reported as mean ± SEM. Data analysis and graphs were built using OriginPro (Origin Lab Corporation, North Hampton, MA, USA). Concentration–response curves were generated by plotting current in the presence of MONIRO-1 ($I_{compound}$) over current prior to application ($I_{control}$) versus a range of MONIRO-1 concentrations tested. Typically, four to six concentrations per channel were screened with five to nine cells per concentration. Concentration–response data were plotted using a rectangular hyperbola assuming a Hill coefficient of 1, using the following expression,

$$(I_{compound}/I_{control}) = 1/(1 + IC_{50}/[drug]),$$

where IC_{50} is the concentration at which half-maximal inhibition was observed.

Steady-state activation and inactivation curves were generated using a modified Boltzmann equation,

$$G = 1/(1 + \exp((Vm - V_{0.5})/\kappa a)),$$

where V_m is the test potential, $V_{0.5}$ is the half-maximal activation potential and κa is the slope factor. SSA and SSI data were each recorded from five to seven individual experiments per channel examined. Recovery from inactivation curves were the results from five to six independent experiments where the complete set of recovery from inactivation time points were acquired. The data were fit using a double exponential of the following equation,

$$I = 1 + A_{fast}{}^{*} \exp(-t/\tau_{fast}) + A_{slow}{}^{*} \exp(-t/\tau_{slow}),$$

where τ is the fast and slow time constant, t is the recovery time and A is the amplitude of the fast and slow time constants. Statistical significance ($P < 0.05$) was determined using unpaired Student's *t*-tests or one-way ANOVA with Tukey's *post hoc* test.

Materials

Compound 2, N-(2-(4-fluorophenoxy)phenyl)-4-(3-guanidinopropoxy)benzamide hydrochloride, MONIRO-1, was synthesized from 2-(4-fluorophenoxy)aniline in four steps, as reported previously (Gleeson *et al.*, 2015). ^{1}H NMR (400 MHz, $CD^{3}OD$): δ 7.88–7.85 (m, 1H), 7.78–7.76 (m, 2H), 7.21–7.18 (m, 2H), 7.07–6.98 (m, 6H), 6.97–6.94 (m, 1H), 4.13 (t, J = 5.9 Hz, 2H), 3.41 (t, J = 6.8 Hz, 2H), 2.11–2.05 (m, 2H). ^{13}C NMR (100 MHz, $CD^{3}OD$): δ 168.2, 163.2, 160.2 (d, J = 239 Hz), 158.7, 154.4, 151.0, 130.5, 130.4, 127.9, 127.6, 126.9, 125.0, 120.8 (d, J = 8.3 Hz), 120.1, 117.2 (d, J = 23.4 Hz), 115.4, 66.3, 39.5, 29.5. ^{19}F NMR (376 MHz, $CD^{3}OD$): δ −120.6, purity >92%, determined by HPLC analysis (λ = 254 nm), all tests were performed using the same batch of compound. The positive control, compound 1 (Z160/NP118809) (Zikolova and Ninov, 1972; Zamponi *et al.*, 2009), was prepared by N-(3-dimethylaminopropyl)-N′-ethylcarbodiimide-assisted acylation of N-benzhydryl piperazine with 3,3-diphenylpropanoic acid. Control compound NNC 55–0396 dihydrochloride was provided by Alomone Labs (Jerusalem, Israel).

Nomenclature of targets and ligands

Key protein targets and ligands in this article are hyperlinked to corresponding entries in http://www.guidetopharmacology.org, the common portal for data from the IUPHAR/BPS Guide to PHARMACOLOGY (Southan *et al.*, 2016), and are permanently archived in the Concise Guide to PHARMACOLOGY 2015/16 (Alexander *et al.*, 2015).

Results

Selective inhibition of human N- and T-type calcium channel subtypes

Whole-cell calcium currents were elicited by depolarizing pulses at a frequency of 0.1 Hz from a holding potential of −80 mV. MONIRO-1 reversibly inhibited channel currents mediated by $Ca_v3.2$ (IC_{50} 1.7 ± 0.1 μM, *n* = 5–9 cells per concentration), $Ca_v3.1$ (IC_{50} 3.3 ± 0.3 μM, *n* = 5–6 cells per concentration), $Ca_v3.3$ (IC_{50} 7.2 ± 0.3 μM, *n* = 5 cells per concentration) and $Ca_v2.2$ (IC_{50} 34.0 ± 3.6 μM, *n* = 5–7 cells per concentration) (Figures 2 and 3A). The effects of MONIRO-1 were further investigated on a panel of VGCCs. At 100 μM, MONIRO-1 had no apparent effect on $Ca_v2.1$ (*n* = 6) or $Ca_v2.3$ (*n* = 5) (Figure 3B) but inhibited $Ca_v1.2$ and $Ca_v1.3$-mediated currents by 46 ± 1% (*n* = 5) and 27 ± 1% (*n* = 5) respectively.

In comparison, Z160/NP118809 (Zamponi *et al.*, 2009) inhibited $Ca_v2.2$-mediated currents with an IC_{50} of 0.28 ± 0.02 μM (*n* = 5–6 cells per concentration), without affecting $Ca_v3.1$ currents (maximal concentration tested 1 μM, Table 1). Application of 10 μM NNC 55-0396, a T-type calcium channel inhibitor, inhibited $hCa_v3.2$ currents by 96 ± 3% (*n* = 5). Furthermore, Z160/NP118809 inhibited **hERG** channels with an IC_{50} of 7.4 μM (Zamponi *et al.*, 2009) whereas 100 μM MONIRO-1 did not inhibit hERG channel-mediated K^{+} currents (Table 1). Table 1 compares the IC_{50} values obtained for MONIRO-1 inhibition of L-, P/Q-, N-, R- and T-type calcium channels and the hERG potassium channel, with that of the control compounds, Z160/NP118809 and **NNC 55-0396**, and other known N- and T-type calcium channel inhibitors where electrophysiology data were obtained across a large portion of the VGCC subtypes.

The current inhibition properties varied between the different MONIRO-1-sensitive Ca_v subtypes, so we analysed the interaction between MONIRO-1 and T-type ($Ca_v3.1$) and N-type ($Ca_v2.2$) calcium channels.

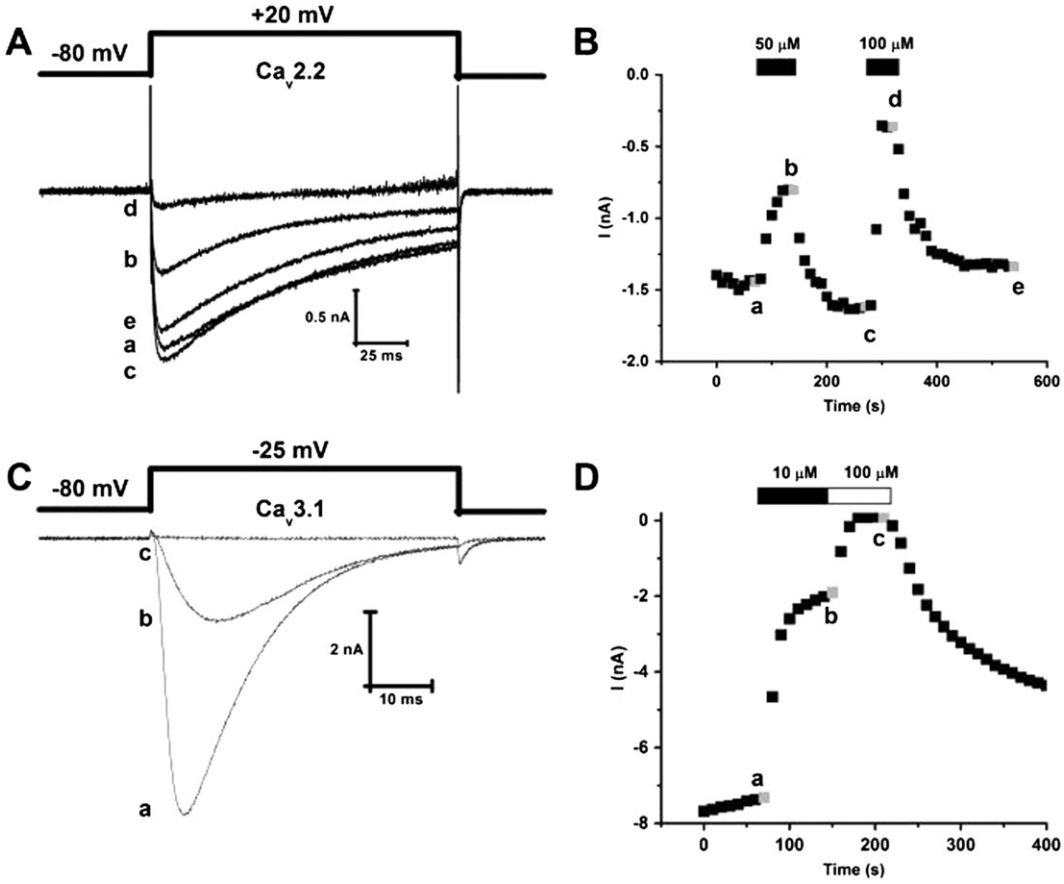

Figure 2

MONIRO-1 inhibition of human $Ca_v2.2$- and $Ca_v3.1$-mediated currents in HEK293 cells. (A) Superimposed whole-cell Ca^{2+} currents recorded from HEK293 cells stably expressing human N-type calcium ($hCa_v2.2$) channels ($\alpha_{1B} + \beta^3 + \alpha^2\delta1$) in response to depolarizing pulses (135 ms duration) to +20 mV from a holding potential of −80 mV. Representative current traces obtained in the absence (a) and presence of 50 (b) and 100 μM (d) MONIRO-1 and after respective washouts (c, e). (B) Peak inward Ca^{2+} current amplitude plotted as a function of time. Time course of inhibition and current amplitude recovery in the presence and following washout of 50 and 100 μM MONIRO-1. Representative currents shown in (A) were obtained at the times indicated by the lower case letters. (C) Superimposed whole-cell Ca^{2+} currents recorded from HEK293 cells transiently expressing human T-type calcium channel, $hCa_v3.1$. These Ca^{2+} currents are in response to depolarizing pulses (50 ms duration) to −25 mV from a holding potential of −80 mV. Representative current traces obtained in the absence (a) and presence of 10 μM (b) and 100 μM (c) MONIRO-1. (D) Peak inward Ca^{2+} current amplitude plotted as a function of time. Time course of inhibition and recovery of current amplitude in the absence (a) and presence of 10 (b) and 100 μM (c) MONIRO-1.

Differential modulation of N- and T-type calcium channels: dependence on frequency and holding potential

We examined the inhibitory characteristics of MONIRO-1 at different test pulse durations and frequencies on $Ca_v2.2$ (Figure 4A, B) and $Ca_v3.1$ channels (Figure 5A, B), as representatives of the VGCC types targeted by MONIRO-1. $Ca_v2.2$ currents in response to shorter (45 ms) depolarizations were 1.5-times more sensitive to MONIRO-1 inhibition than those elicited by a longer (135 ms) pulse. Channels held open by the longer pulse also recovered more completely from block (82 ± 9%, n = 5) than those briefly opened (45 ms; 47 ± 3%, n = 5) (Figure 4A). In agreement with these findings, higher frequency stimulation of $Ca_v2.2$ channels rendered a population of channels that was more potently inhibited by MONIRO-1 (0.03, 0.1 and 0.2 Hz; Figure 4B). At a frequency of 0.2 Hz, MONIRO-1 inhibited $Ca_v2.2$ current by 29 ± 1% (n = 5), whereas at 0.1 and 0.03 Hz, only 21 ± 1% (n = 5) and 16 ± 1% (n = 5) of the current amplitude was inhibited respectively. Interestingly, the effects of MONIRO-1 on $Ca_v2.2$ channels are in marked contrast to its effects on $Ca_v3.1$ channels (Figure 5A, B). In the case of $Ca_v3.1$ channels, pulse duration did not affect $Ca_v3.1$-mediated current inhibition (% block 15 ms: 43 ± 3%, n = 5; and 50 ms: 51 ± 7%, n = 5), recovery from inhibition (% recovery 15 ms: 95 ± 1.3%, n = 5; and 50 ms: 99 ± 0.8%, n = 5) or frequency dependence of block over the same range as those tested for $Ca_v2.2$ channels (% block at 0.2 Hz = 43 ± 1.5%, n = 5; 0.1 Hz = 42 ± 2.3%, n = 5; and 0.03 Hz = 44 ± 1.6%, n = 5). However, at faster rates of 1 and 2 Hz, there was a significant increase in MONIRO-1 block of $Ca_v3.1$ channels (% block at 1 Hz = 61.0 ± 1.5%, n = 6; and 2 Hz = 71.0 ± 2.0%, n = 5). This would increase threefold the affinity for channels firing at faster frequencies of 2 Hz compared with those firing at rates <0.2 Hz.

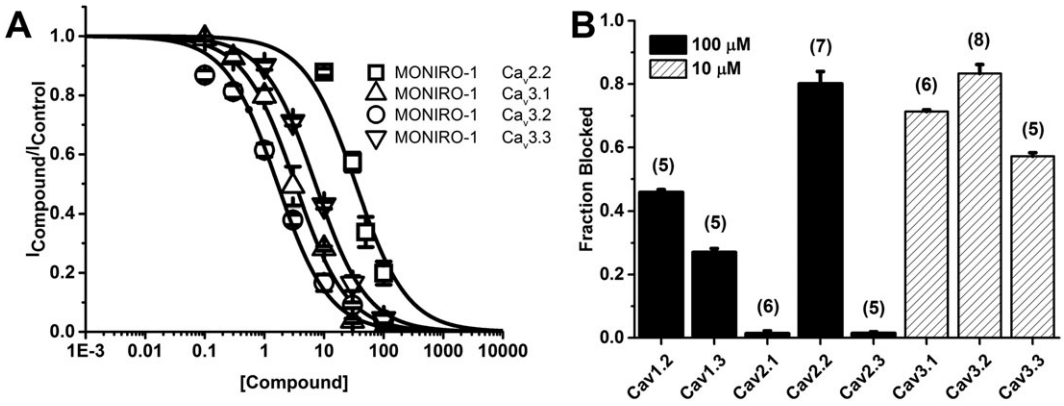

Figure 3

MONIRO-1 inhibition of voltage-gated calcium channels. (A) Concentration–response of MONIRO-1 at hCa$_v$2.2, hCa$_v$3.1, hCa$_v$3.2 and hCa$_v$3.3 channels expressed in HEK293 cells. Fitted curves gave IC_{50} values as shown in the Results. (B) Fraction of current inhibited by 100 (solid) or 10 μM (striped) MONIRO-1 at Ca$_v$1.3, Ca$_v$2.1, Ca$_v$2.2, Ca$_v$2.3, Ca$_v$3.1 and Ca$_v$3.2 channels. Cells were held at −80 mV and pulsed at 0.1 Hz to the voltage determined to elicit the peak inward current previously determined from an I–V protocol. The number of cells is indicated in parentheses.

Table 1

Comparison of IC_{50} values obtained for MONIRO-1 inhibition of L-, P/Q-, N-, R- and T-type calcium channels and the hERG potassium channel, with control compounds Z160/NP118809 and NNC 55-0396 and other known N- and T-type calcium channel inhibitors

	L-type (μM)	P/Q-type (μM)	N-type (μM)	R-type (μM)	T-type (μM)	hERG (μM)
Z160/NP118809 (Zamponi *et al.*, 2009)	12[b] (Ca$_v$1.2)	–	0.28[a]	–	–	7.4[b]
[a]MONIRO-1	27% @ 100 (Ca$_v$1.3) 46% @ 100 (Ca$_v$1.2)	>100	34	>100	3.3 (Ca$_v$3.1) 1.7 (Ca$_v$3.2) 7.2 (Ca$_v$3.3)	>100
A-1048400 (Scott *et al.*, 2012)	28	1.3	0.8	–	0.9 (Ca$_v$3.2)	–
Z944 (Tringham *et al.*, 2012)	32 (Ca$_v$1.2)	–	11	–	0.05 (Ca$_v$3.1) 0.16 (Ca$_v$3.2)	7.8
NNC 55–0396 (Chen *et al.*, 2014)	–	–	–	–	6.8[b] (Ca$_v$3.1) 96% @10[a] (Ca$_v$3.2)	–
Ziconotide (Wang *et al.*, 2016)	–	>10	0.18[b]	–	–	–
TTA-A2 (Kraus *et al.*, 2010)	>30[b] (Ca$_v$1.2)	>30[b]	>30[b]Recovery from block	>30[b]	0.09 (Ca$_v$3.1) 0.09 (Ca$_v$3.2)	–
TROX-1 (Swensen *et al.*, 2012)	–	0.29	0.19	0.28	–	–

[a]This work.
[b]Studies were performed with HEK293 cells stably expressing the desired voltage-gated calcium channel. –, not tested.

To further explore the differential effects of MONIRO-1 on Ca$_v$2.2 and Ca$_v$3.1 channels, we investigated the effect of membrane holding potential on block of Ca$_v$2.2 and Ca$_v$3.1 channels. MONIRO-1 could more effectively block Ca$_v$2.2 channels at more depolarized potentials (block at −100 mV = 34 ± 1.8%; −80 mV = 43 ± 3.2%; and −60 mV = 77 ± 5.5%, n = 5). In contrast, block at all of the holding potentials tested did not affect the degree by which MONIRO-1 inhibited Ca$_v$3.1 channels (block at −100 mV = 41-± 0.5%; −80 mV = 46 ± 5.1%; and −60 mV = 43 ± 0.6%, n = 5) (Figures 4C and 5C). This result highlights the state-dependent differences between MONIRO-1 inhibition of Ca$_v$2.2 and Ca$_v$3.1 channels.

Effects of MONIRO-1 on N- and T-type calcium channel activation, inactivation and recovery from inactivation

To identify any effects that MONIRO-1 may have on calcium current kinetics and to understand the mechanisms behind

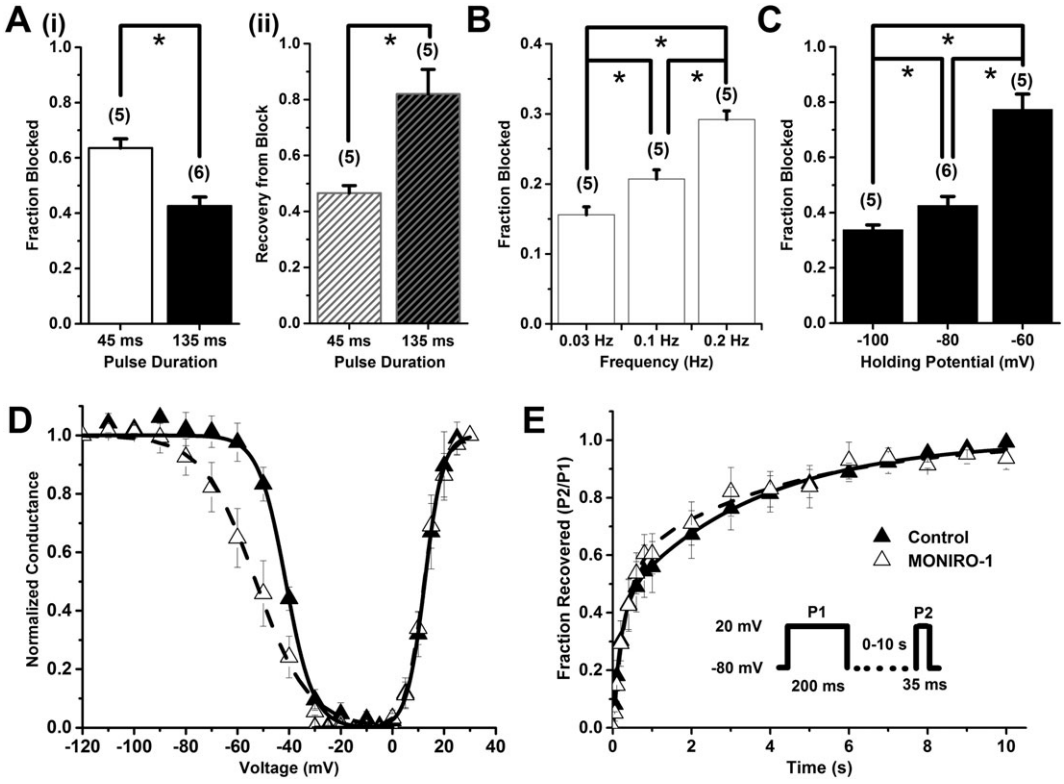

Figure 4

MONIRO-1 block of human $Ca_v2.2$ channels. (A) (i) Fraction blocked and (ii) recovery from block by 30 μM MONIRO-1, with a depolarizing pulse duration of 45 ms or 135 ms, from a holding potential of −80 mV to a test potential that elicits maximal inward current, repeated every 10 s. The number of cells is indicated in parentheses. (B) Fraction of current inhibited by 10 μM MONIRO-1 at three different frequencies (0.03, 0.1 and 0.2 Hz; holding potential −80 mV). The number of cells is indicated in parentheses. (C) Effect of holding potential (−100, −80 and −60 mV) on the fraction of current blocked by 30 μM MONIRO-1 (pulsed at 0.1 Hz). The number of cells is indicated in parentheses. (D) Activation and SSI curves in the absence (control) and presence of 30 μM MONIRO-1. Activation curves were generated through indicated depolarizing test pulses (135 ms) from a holding potential of −80 mV, repeated every 10 s. For SSI curves, selected pre-pulse potentials (−120 to 0 mV in 5 mV increments for 10 s) were applied prior to a test pulse (135 ms) determined from the peak current, repeated every 15 s from a holding potential of −80 mV. (E) Recovery from inactivation in the absence (control) and presence of 30 μM MONIRO-1. A two-pulse protocol (Inset) was repeated every 15 s, where the time was varied between the first fully inactivating pulse and the test pulse (0–10 s). *$P < 0.05$, significantly different as indicated; n.s. = not significant; Student's *t*-test.

the enhanced inhibition at depolarised membrane potentials, we examined its effects at half-maximal concentrations on $Ca_v2.2$ and $Ca_v3.1$ activation and SSI (Figures 4D and 5D). Exposure to MONIRO-1 did not affect the voltage-dependence of activation of $Ca_v2.2$ or $Ca_v3.1$ channels (Table 2). However, there was a significant ~10 mV hyperpolarizing shift in $Ca_v2.2$ SSI. An apparent decrease in the voltage-dependence of SSI was also seen. However, no significant changes were observed in $Ca_v3.1$ SSI in the presence of MONIRO-1 or voltage-dependence of SSI. Channel activation and inactivation time constants were examined, with and without MONIRO-1, for $Ca_v2.2$ (30 μM) and $Ca_v3.1$ channels (3 μM). MONIRO-1 had no effect on either the activation or inactivation time constants of $Ca_v2.2$ channels (Table 2). However, MONIRO-1 application increased both activation and inactivation time constants for $Ca_v3.1$ channels (Table 2).

Finally, we investigated the effect of MONIRO-1 on $Ca_v2.2$ and $Ca_v3.1$ channel recovery from inactivation. MONIRO-1 had no observed effect on $Ca_v2.2$ recovery from inactivation time constants or their relative contribution to either time constants (control τ_{fast} = 0.22 ± 0.1 s, A_{fast} = 57 ± 8.5%; τ_{slow} = 2.8 ± 0.7 s, A_{slow} = 45 ± 8.6%; MONIRO-1 τ_{fast} = 0.14 ± 0.1 s, A_{fast} = 43 ± 7.0%; τ_{slow} = 2.4 ± 0.4 s, A_{slow} = 58 ± 6.2%, n = 5 respectively). However, MONIRO-1 slowed recovery of $Ca_v3.1$ channels from inactivation by decreasing the relative contribution of the fast recovery time constant while increasing the contribution of the slow time constant (control τ_{fast} = 0.051 ± 0.008 s, A_{fast} = 80.1 ± 5.1%; τ_{slow} = 0.20 ± 0.11 s, A_{slow} = 21.8 ± 5.4%; MONIRO-1 τ_{fast} = 0.026 ± 0.007 s, A_{fast} = 29.6 ± 4.2%; τ_{slow} = 0.33 ± 0.03 s, A_{slow} = 70 ± 4.1%, n = 6; $P < 0.05$). Therefore, MONIRO-1 can inhibit $Ca_v3.1$ channels more efficiently at firing frequencies >1 Hz (Figure 5B), as indicated by the slowed recovery from inactivation and frequency dependence, such as those prevailing in hyperexcitable neurons (Cain and Snutch, 2010).

Discussion

In this study, we examined the effects of an *ortho*-phenoxyanilide on the inhibition and biophysical properties of VGCCs. This *ortho*-phenoxyanilide, MONIRO-1, is a low

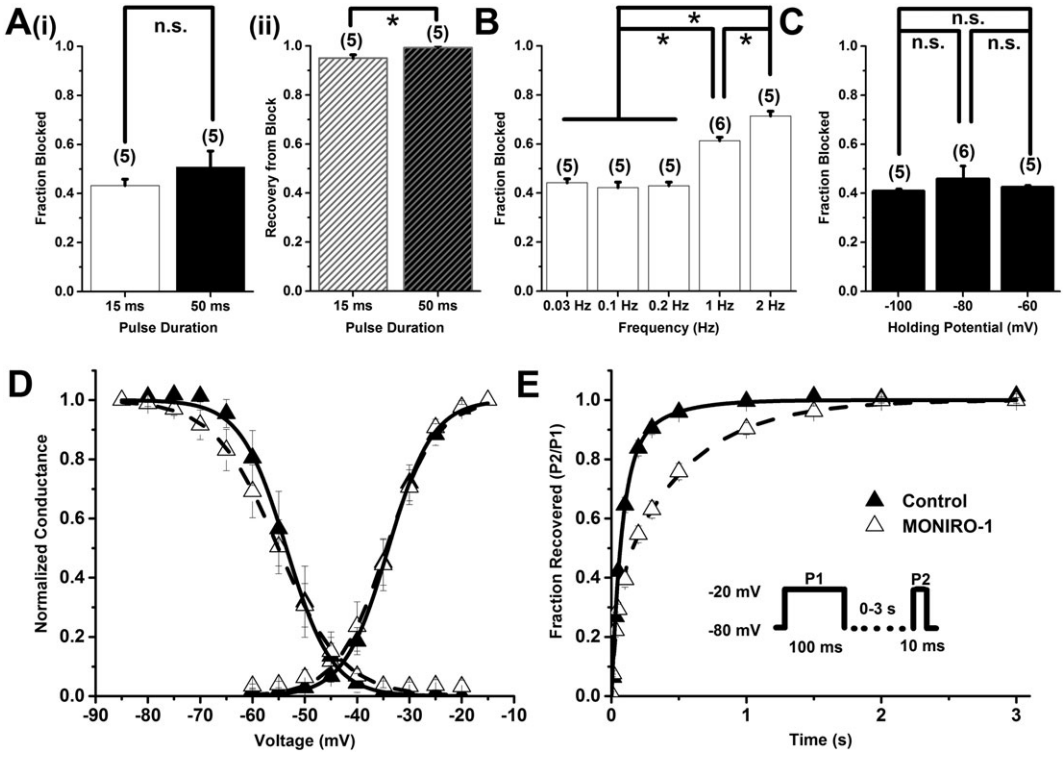

Figure 5

MONIRO-1 block of human $Ca_v3.1$ channels. (A) (i) Bar graph showing fraction blocked and (ii) recovery from block by 3 μM MONIRO-1, with a depolarizing pulse duration of 15 ms or 50 ms, from a holding potential of −80 mV repeated every 10 s. The number of cells is indicated in parentheses. (B) Bar graph of the fractional current inhibited by 3 μM MONIRO-1 at five different frequencies (0.03, 0.1, 0.2, 1 and 2 Hz; holding potential −80 mV). The number of cells is indicated in parentheses. (C) Effect of holding potential (−100, −80 and −60 mV) on the fraction of current inhibited by 3 μM MONIRO-1 (pulsed at 0.1 Hz). The number of cells is indicated in parentheses. (D) Activation and SSI curves in the absence (control) and presence of 3 μM MONIRO-1. Activation curves were generated through indicated depolarizing test pulses (50 ms) from a holding potential of −80 mV, repeated every 10 s. For SSI curves, selected pre-pulse potential values (−85 to −20 mV in 5 mV increments for 1 s) were applied prior to a test pulse (50 ms) determined from the peak current, repeated every 10 s from a holding potential of −80 mV. (E) Recovery from inactivation in the absence (control) and presence of 3 μM MONIRO-1. A two-pulse protocol (Inset) was repeated every 15 s, where the time was varied between the first fully inactivating pulse and the test pulse. *$P < 0.05$, significantly different as indicated; n.s. = not significant; Student's *t*-test.

Table 2

Comparison of activation and inactivation parameters between $Ca_v2.2$ and $Ca_v3.1$ channels before and after application of MONIRO-1

	$Ca_v2.2$		$Ca_v3.1$	
	Control	MONIRO-1 (30 μM)[a]	Control	MONIRO-1 (3 μM)[a]
τ activation	1.81 ± 0.15 ms (5)	1.51 ± 0.17 ms (5)	1.90 ± 0.08 ms (5)	3.45 ± 0.51 ms (5)*
τ inactivation	61.75 ± 13.69 ms (5)	44.45 ± 7.61 ms (5)	10.78 ± 0.52 ms (5)	17.91 ± 0.74 ms (5)*
$V_{0.5}$ activation	12.5 ± 0.5 mV (5)	12.4 ± 0.4 mV (5)	−34.0 ± 0.4 mV (7)	−34.4 ± 0.6 mV (7)
$V_{0.5}$ inactivation	−41.3 ± 0.7 mV (5)	−52.9 ± 1.3 mV (5)*	−53.5 ± 0.6 mV (6)	−55.1 ± 0.6 mV (6)
Slope factor	5.3 ± 0.6 (5)	10.2 ± 1.2 (5)*	4.4 ± 0.6 (6)	6.1 ± 0.5 (6)

*$P < 0.05$ compared with control, Students *t*-test. Data presented as mean ± SEM and n is given in brackets.
[a]Concentration chosen based on IC_{50} of individual channel.

MW compound and was selected for its ability to inhibit VGCCs in a high-throughput calcium influx assay (Gleeson *et al.*, 2015). To ascertain its selectivity and mode of action, we examined its potency of block and biophysical properties on a variety of VGCCs. MONIRO-1 was shown to be an N- and T-type calcium channel inhibitor with advantageous biophysical properties, including state- and use-dependence. It specifically targets $Ca_v3.2$ and $Ca_v2.2$ channels, which have

been implicated in various pain pathways, and $Ca_v3.1$ channels, which are involved in cell signalling and epilepsy (Choi, 2013; Waxman and Zamponi, 2014).

Given that MONIRO-1 inhibits depolarization-activated calcium responses from SH-SY5Y cells (Gleeson *et al.,* 2015), we determined its efficacy and selectivity against several VGCCs expressed in HEK293 cells. After screening representative members of each VGCC family (L-, N-, P/Q-, R- and T-types), we established that MONIRO-1 preferentially inhibits T-type channels ($Ca_v3.1$, $Ca_v3.2$ and $Ca_v3.3$ channels), modestly interacts with N-type $Ca_v2.2$ channels (with 5–20 times less affinity compared to T-type calcium channels) and has poor efficacy for L-type ($Ca_v1.2$ and $Ca_v1.3$ channels $IC_{50} > 100$ μM). No other VGCCs investigated (P/Q-type $Ca_v2.1$; R-type $Ca_v2.3$) responded to high concentrations of MONIRO-1. hERG, a typical off-target channel for low MW compounds, was not modulated by MONIRO-1 at concentrations up to 100 μM. Subsequently, we characterized the mechanism of MONIRO-1 inhibition on its primary targets, N- and T-type calcium channels.

In the present study, MONIRO-1 inhibited $Ca_v3.1$ channels with an IC_{50} of 3 μM, so we examined the mechanistic details of this inhibition. Many T-type calcium channel inhibitors have been identified in assays looking for inactivation state-dependent inhibitors. These studies have led to compounds that predominantly bind and alter SSI, including TTA-A2, A-1048400 and NNC 55-0396, unlike MONIRO-1, which does not affect SSI of $Ca_v3.1$ channels. MONIRO-1 (3 μM) significantly slowed both channel activation and inactivation kinetics, without discernible effects on either $V_{0.5act}$ or $V_{0.5inact}$. MONIRO-1 slowed recovery of $Ca_v3.1$ from inactivation at rates >1 Hz, which was reflected as an increase in current inhibition at 1 and 2 Hz (Figure 5B, E), suggesting that MONIRO-1 would preferentially target epileptic firing neurons over normal firing neurons. Taken together, the lack of effect of MONIRO-1 on other biophysical properties examined, including the lack of effect of holding potential, suggests that it acts by binding to prevent $Ca_v3.1$ channels from transitioning from a non-conducting state to the open state. Therefore, the prolonged recovery from inactivation caused by MONIRO-1 inhibition of $Ca_v3.1$-mediated currents is likely to be due to the slower dissociation of the compound from the open-blocked channels or due to its accelerating channel transitions into a slow inactivated channel conformation. A similar phenomenon has been observed for mibefradil inhibition of $Ca_v2.1$ channels (Timin *et al.,* 2004).

$Ca_v3.1$ channels are key players in the circuitry involved in sleep including the reticular thalamic nucleus, thalamic relay neurons and neocortical pyramidal cells (Chen *et al.,* 2014). $Ca_v3.1$ channels are highly expressed in thalamocortical neurons (Kim *et al.,* 2001; Song *et al.,* 2004), where they initiate entry of these neurons into bursting mode – a typical activity mode in absence seizures (Cain and Snutch, 2013). Consequently, $Ca_v3.1$ channels have been directly linked to absence of epilepsies (Kim *et al.,* 2001). Disease mutations in $Ca_v3.2$ channels have also been linked to both rat models and human idiopathic generalized epilepsy (Khosravani *et al.,* 2005; Powell *et al.,* 2009), suggesting that inhibitors of both $Ca_v3.1$ and $Ca_v3.2$ channels could decrease neuronal firing induced by hyperactivity of these channels during epilepsy. Compound Z944, which has higher affinity for the inactivated state of T-type calcium channels over the resting state, reduced seizure activity in terms of time spent in seizure and the total number of seizures per hour (Tringham *et al.,* 2012). During burst firing, VGCCs repetitively open and close at frequencies of 5–10 Hz (Cain and Snutch, 2010). Ideally, an anti-epileptogenic drug targeting $Ca_v3.1$ or $Ca_v3.2$ channels in epileptogenic foci, that is, on neurons in bursting mode where the channels are in the open state. Our results suggest that MONIRO-1 modulates $Ca_v3.1$ channels by holding the channel in a non-conducting state, thus prolonging recovery from inactivation, which makes the compound well suited for the study and/or potentially for the amelioration of $Ca_v3.1$ or $Ca_v3.2$-mediated epileptogenesis in neurons entering bursting mode.

Considerable research into pain physiology has focused on voltage-gated N- and T-type calcium channels. $Ca_v3.2$ channels are expressed in peripheral sensory neurons, where they modulate pain processing by controlling dorsal root ganglion neuroexcitability (Carbone and Lux, 1984). $Ca_v2.2$ channels are located at presynaptic terminals in the CNS, where they modulate neurotransmitter release and fast synaptic transmission (Wheeler *et al.,* 1994). MONIRO-1 inhibits $Ca_v2.2$ channels under resting state conditions with an IC_{50} of ~30 μM, which is approximately 10-fold higher than that observed the T-type channels. However, the effect of MONIRO-1 on $Ca_v2.2$ channels is enhanced at higher frequencies, where faster pacing of the channel increased inhibition. At frequencies as high as 0.2 Hz (the maximum tested), the apparent affinity increased to ~20 μM, with no observable change to the time course of activation or inactivation of the channel (Figure 4B and Table 2).

Following this observation, we examined the potential state dependence of the activity of MONIRO-1. Short (45 ms) depolarizing test pulses produced greater inhibition of $Ca_v2.2$ channels as well as less recovery after washout compared with a longer (135 ms) test pulse, suggesting a possible decrease in affinity for the open and/or inactivated state (Figure 4A). MONIRO-1 had a pronounced effect on $Ca_v2.2$ channel SSI that was not paralleled in $Ca_v3.1$ channels (Figure 4D), along with strong dependence on holding potential. At −60 mV, ~80% of the whole-cell current was inhibited compared with −100 mV where only ~35% of the current was blocked (Figure 4C). Such a hyperpolarizing shift in SSI and the dependence on holding potential suggests that MONIRO-1 preferentially binds to the inactivated state of N-type calcium channels (Bean *et al.,* 1983; Bean, 1984; Sanguinetti and Kass, 1984). Interestingly, unlike its effect on T-type calcium channels, MONIRO-1 did not influence N-type calcium channel recovery from inactivation (Figure 5E), suggesting a distinct mode of action against the two channel families.

Nociceptive stimuli cause depolarization, calcium channel opening, intracellular $[Ca^{2+}]$ increase and neuronal hyper-excitability, as shown by faster firing rates (Winquist *et al.,* 2005). Nociceptive stimuli reduce the effective open time and increase the frequency of channel opening (Winquist *et al.,* 2005). Sustained neuronal firing in pain syndromes increases cytosolic calcium levels in the dorsal horn and shifts calcium channels into the inactivated state. Therefore, drugs that target $Ca_v2.2$ channels are best suited to 'prefer' those channels in the inactivated state

(predominant in pain syndromes), allowing normal neurotransmitter release signalled by these channels in neurons not in a pain state.

A few compounds have recently reported to exhibit use- and/or state-dependent inhibition of calcium channels involved in pain signalling, including A-1048400 (Scott *et al.,* 2012) (compound **3**, Figure 1), Z160/NP118809 **1** (Zamponi *et al.,* 2009) and **TROX-1** (Abbadie *et al.,* 2010). To explore MONIRO-1 inhibitory mechanism of $Ca_v2.2$, we examined stimulation conditions comparable with those occurring in the physiological setting. Given that $Ca_v2.2$ channels can potentially accumulate in the inactivated state in hyperactive pain state conditions (Winquist *et al.,* 2005), the selective effect of MONIRO-1 on channels in this state could be a valuable pharmacological property that would enable therapeutic targeting during neuropathic pain treatment. Frequency dependence and preference of MONIRO-1 for the inactivated $Ca_v2.2$ channels suggest that it or related compounds may prove useful in the prevention of high-frequency firing episodes, an important signalling mode occurring during pain transmission. Therefore, MONIRO-1 may preferentially inhibit channels in hyperexcitable states in pain-specific loci, leaving normally firing neurons unaffected (Liao *et al.,* 2011).

In conclusion, we have identified MONIRO-1 as a low MW antagonist of voltage-gated calcium channels with 10- to 100-fold higher affinity for $Ca_v3.1$, $Ca_v3.2$, $Ca_v3.3$ and $Ca_v2.2$ channels than other classes of VGCCs examined. MONIRO-1 is a valuable tool for the study of VGCCs because it inhibits N- and T-type calcium channels through distinct mechanisms. Given its state- and use-dependent inhibition of $Ca_v2.2$ channels (preferentially inhibits the inactivated state) and $Ca_v3.1$ channels (prohibiting channel transitions to the open state), while exhibiting frequency-dependent block of both channels, MONIRO-1 is a novel lead compound that could be used to develop Ca_v channel blockers to treat VGCC pathologies, including neuropathic pain and epilepsy. MONIRO-1 shows a novel mechanism of block of hCav3.1 channels compared with previously described T-type calcium channel blockers, in that it slows channel activation and inactivation kinetics and traps channels at high-frequency firing (>1 Hz) from transitioning to the open state while not altering SSI. Prior to *in vivo* assess*ment of* their analgesic potential, MONIRO-1 and analogues need to be characterized at other voltage-gated ion channels in pain pathways, including $Na_v1.7$ and $Na_v1.8$ channels.

Acknowledgements

We thank Dr J. E. Graham for helping with chemical synthesis and Dr. R. K. Finol-Urdaneta for providing valuable comments on drafts of the manuscript. This work was funded by a National Health and Medical Research Council (NHMRC) Program Grant awarded to D.J.A. and R.J.L. (APP1072113). The Monash–CSIRO Collaborative Research Support Scheme and CSIRO's Australian Biotech Growth Partnerships Theme also helped to fund this research.

Author contributions

J.R.M., P.J.D., K.L.T. and D.J.A. designed the experiments; J.R.M., L.M., E.C.G. and S.S. performed the experiments; J.R.M. analysed the electrophysiological data; J.R.M., P.J.D., K.L.T. and D.J.A. prepared the figures; J.R.M. wrote the manuscript; J.R.M., R.J.L., P.J.D., K.L.T. and D.J.A. revised the manuscript. All authors reviewed the manuscript.

Conflict of interest

The authors declare no conflicts of interest.

Declaration of transparency and scientific rigour

This Declaration acknowledges that this paper adheres to the principles for transparent reporting and scientific rigour of preclinical research recommended by funding agencies, publishers and other organisations engaged with supporting research.

References

Abbadie C, McManus OB, Sun S-Y, Bugianesi RM, Dai G, Haedo RJ *et al.* (2010). Analgesic effects of a substituted N-triazole oxindole (TROX-1), a state-dependent, voltage-gated calcium channel 2 blocker. J Pharmacol Exp Ther 334: 545–555.

Alexander SPH, Peters JA, Kelly E, Marrion N, Benson HE, Faccenda E *et al.* (2015). The Concise Guide to PHARMACOLOGY 2015/16: Voltage-gated ion channels. Br J Pharmacol 172: 5904–5941.

Altier C, Zamponi GW (2004). Targeting Ca^{2+} channels to treat pain: T-type versus N-type. Trends Pharmacol Sci 25: 465–470.

Andersson A, Baell JB, Duggan PJ, Graham JE, Lewis RJ, Lumsden NG *et al.* (2009). ω-Conotoxin GVIA mimetics based on an anthranilamide core: effect of variation in ammonium side chain lengths and incorporation of fluorine. Bioorg Med Chem 17: 6659–6670.

Baell JB, Duggan PJ, Forsyth SA, Lewis RJ, Lok YP, Schroeder CI (2004). Synthesis and biological evaluation of nonpeptide mimetics of ω-conotoxin GVIA. Bioorg Med Chem 12: 4025–4037.

Baell JB, Duggan PJ, Forsyth SA, Lewis RJ, Lok YP, Schroeder CI *et al.* (2006). Synthesis and biological evaluation of anthranilamide-based non-peptide mimetics of ω-conotoxin GVIA. Tetrahedron 62: 7284–7292.

Bean BP (1984). Nitrendipine block of cardiac calcium channels: high-affinity binding to the inactivated state. Proc Natl Acad Sci U S A 81: 6388–6392.

Bean BP, Cohen CJ, Tsien RW (1983). Lidocaine block of cardiac sodium channels. J Gen Physiol 81: 613–642.

Bladen C, McDaniel SW, Gadotti VM, Petrov RR, Berger ND, Diaz P *et al.* (2015). Characterization of novel cannabinoid based T-type calcium channel blockers with analgesic effects. ACS Chem Nerosci 6: 277–287.

Bourinet E, Alloui A, Monteil A, Barrere C, Couette B, Poirot O *et al.* (2005). Silencing of the $Ca_v3.2$ T-type calcium channel gene in sensory neurons demonstrates its major role in nociception. EMBO J 24: 315–324.

Bourinet E, Altier C, Hildebrand ME, Trang T, Salter MW, Zamponi GW (2014). Calcium-permeable ion channels in pain signaling. Physiol Rev 94: 81–140.

Butterworth JF, Strichartz GR (1990). Molecular mechanisms of local anesthesia: a review. Anesthesiology 72: 711–734.

Cain SM, Snutch TP (2010). Contributions of T-type calcium channel isoforms to neuronal firing. Channels 4: 475–482.

Cain SM, Snutch TP (2013). T-type calcium channels in burst-firing, network synchrony, and epilepsy. Biochimica et Biophysica Acta (BBA) - Biomembranes 1828: 1572–1578.

Carbone E, Lux HD (1984). A low voltage-activated, fully inactivating Ca channel in vertebrate sensory neurones. Nature 310: 501–502.

Catterall WA, Perez-Reyes E, Snutch TP, Striessnig J (2005). International union of pharmacology. XLVIII. Nomenclature and structure-function relationships of voltage-gated calcium channels. Pharmacol Rev 57: 411–425.

Chen Y, Chen Y, Parker WD, Wang K (2014). The role of T-type calcium channel genes in absence seizures. Front Neurol 5: 1–8.

Cheong E, Shin H-S (2013). T-type Ca^{2+} channels in normal and abnormal brain functions. Physiol Rev 93: 961–992.

Choi K-H (2013). The design and discovery of T-type calcium channel inhibitors for the treatment of central nervous system disorders. Expert Opin Drug Discov 8: 919–931.

Choi S, Na HS, Kim J, Lee J, Lee S, Kim D *et al.* (2007). Attenuated pain responses in mice lacking $Ca_v3.2$ T-type channels. Genes Brain Behav 6: 425–431.

Chouabe C, Drici M-D, Romey G, Barhanin J, Lazdunski M (1998). HERG and KvLQT1/IsK, the cardiac K^+ channels involved in long QT syndromes, are targets for calcium channel blockers. Mol Pharmacol 54: 695–703.

Curtis MJ, Bond RA, Spina D, Ahluwalia A, Alexander SP, Giembycz MA *et al.* (2015). Experimental design and analysis and their reporting: new guidance for publication in BJP. Br J Pharmacol 172: 3461–3471.

Dai G, Haedo RJ, Warren VA, Ratliff KS, Bugianesi RM, Rush A *et al.* (2008). A high-throughput assay for evaluating state dependence and subtype selectivity of Ca_v2 calcium channel inhibitors. Assay Drug Dev Technol 6: 195–212.

Duggan PJ, Lewis RJ, Phei Lok Y, Lumsden NG, Tuck KL, Yang A (2009). Low molecular weight non-peptide mimics of ω-conotoxin GVIA. Bioorg Med Chem Lett 19: 2763–2765.

Eller P, Berjukov S, Wanner S, Huber I, Hering S, Knaus HG *et al.* (2000). High affinity interaction of mibefradil with voltage-gated calcium and sodium channels. Br J Pharmacol 130: 669–677.

Flatters SJL, Bennett GJ (2004). Ethosuximide reverses paclitaxel- and vincristine-induced painful peripheral neuropathy. Pain 109: 150–161.

Francois A, Kerckhove N, Meleine M, Alloui A, Barrere C, Gelot A *et al.* (2013). State-dependent properties of a new T-type calcium channel blocker enhance $Ca_V3.2$ selectivity and support analgesic effects. Pain 154: 283–293.

François A, Laffray S, Pizzoccaro A, Eschalier A, Bourinet E (2014). T-type calcium channels in chronic pain: mouse models and specific blockers. Pflugers Arch - Eur J Physiol 466: 707–717.

Gleeson EC, Graham JE, Spiller S, Vetter I, Lewis RJ, Duggan PJ *et al.* (2015). Inhibition of N-Type calcium channels by fluorophenoxyanilide derivatives. Mar Drugs 13: 2030–2045.

Gold MS, Gebhart GF (2010). Nociceptor sensitization in pain pathogenesis. Nat Med 16: 1248–1257.

Gomora JC, Murbartian J, Arias JM, Lee JH, Perez-Reyes E (2002). Cloning and expression of the human T-type channel $Ca_V3.3$: insights into prepulse facilitation. Biophys J 83: 229–241.

Guo D, Hu J (2014). Spinal presynaptic inhibition in pain control. Neuroscience 283: 95–106.

Helton TD, Xu W, Lipscombe D (2005). Neuronal L-type calcium channels open quickly and are inhibited slowly. J Neurosci 25: 10247–10251.

Hondeghem LM, Katzung BG (1984). Antiarrhythmic agents: the modulated receptor mechanism of action of sodium and calcium channel-blocking drugs. Annu Rev Pharmacol Toxicol 24: 387–423.

Khosravani H, Bladen C, Parker DB, Snutch TP, McRory JE, Zamponi GW (2005). Effects of $Ca_V3.2$ channel mutations linked to idiopathic generalized epilepsy. Ann Neurol 57: 745–749.

Kim D, Song I, Keum S, Lee T, Jeong M-J, Kim S-S *et al.* (2001). Lack of the burst firing of thalamocortical relay neurons and resistance to absence seizures in mice lacking α1G T-Type Ca^{2+} channels. Neuron 31: 35–45.

Kraus RL, Li Y, Gregan Y, Gotter AL, Uebele VN, Fox SV*et al.* (2010). In vitro characterization of T-type calcium channel antagonist TTA-A2 and in vivo effects on arousal in mice. J Pharmacol Exp Ther 335: 409–417.

Lee MS (2014). Chapter Four – recent progress in the discovery and development of N-type calcium channel modulators for the treatment of pain. In: Lawton G, Witty DR (eds). Prog Med Chem. Elsevier: Oxford, UK, pp. 147–186.

Lee S (2013). Pharmacological inhibition of voltage-gated Ca^{2+} channels for chronic pain relief. Curr Neuropharm 11: 606–620.

Liao Y-F, Tsai M-L, Chen C-C, Yen C-T (2011). Involvement of the $Ca_v3.2$ T-type calcium channel in thalamic neuron discharge patterns. Mol Pain 7: 43.

Matthews EA, Dickenson AH (2001). Effects of ethosuximide, a T-type Ca^{2+} channel blocker, on dorsal horn neuronal responses in rats. Eur J Pharmacol 415: 141–149.

McCleskey EW, Fox AP, Feldman DH, Cruz LJ, Olivera BM, Tsien RW *et al.* (1987). ω-Conotoxin: direct and persistent blockade of specific types of calcium channels in neurons but not muscle. Proc Natl Acad Sci U S A 84: 4327–4331.

Nilius B, Prenen J, Voets T, Eggermont J, Droogmans G (1998). Activation of volume-regulated chloride currents by reduction of intracellular ionic strength in bovine endothelial cells. J Physiol 506: 353–361.

Perret D, Luo ZD (2009). Targeting voltage-gated calcium channels for neuropathic pain management. Neurotherapeutics 6: 679–692.

Pope JE, Deer TR (2013). Ziconotide: a clinical update and pharmacologic review. Expert Opin Pharmacother 14: 957–966.

Powell KL, Cain SM, Ng C, Sirdesai S, David LS, Kyi M *et al.* (2009). A $Ca_V3.2$ T-type calcium channel point mutation has splice-variant-specific effects on function and segregates with seizure expression in a polygenic rat model of absence epilepsy. J Neurosci 29: 371–380.

Reger TS, Yang Z-Q, Schlegel K-AS, Shu Y, Mattern C, Cube R *et al.* (2011). Pyridyl amides as potent inhibitors of T-type calcium channels. Bioorg Med Chem Lett 21: 1692–1696.

Saegusa H, Kurihara T, Zong S, Kazuno A-A, Matsuda Y, Nonaka T *et al.* (2001). Suppression of inflammatory and neuropathic pain symptoms in mice lacking the N-type Ca^{2+} channel. EMBO J 20: 2349–2356.

Sanguinetti MC, Kass RS (1984). Voltage-dependent block of calcium channel current in the calf cardiac Purkinje fiber by dihydropyridine calcium channel antagonists. Circ Res 55: 336–348.

Scott VE, Vortherms TA, Niforatos W, Swensen AM, Neelands T, Milicic I *et al.* (2012). A-1048400 is a novel, orally active, state-dependent neuronal calcium channel blocker that produces dose-dependent antinociception without altering hemodynamic function in rats. Biochem Pharmacol 83: 406–418.

Sekiguchi F, Kawabata A (2013). T-type calcium channels: functional regulation and implication in pain signaling. J Pharmacol Sci 122: 244–250.

Simms BA, Zamponi GW (2014). Neuronal voltage-gated calcium channels: structure, function, and dysfunction. Neuron 82: 24–45.

Song I, Kim D, Choi S, Sun M, Kim Y, Shin H-S (2004). Role of the α1G T-type calcium channel in spontaneous absence seizures in mutant mice. J Neurosci 24: 5249–5257.

Southan C, Sharman JL, Benson HE, Faccenda E, Pawson AJ, Alexander SP *et al.* (2016). The IUPHAR/BPS guide to PHARMACOLOGY in 2016: towards curated quantitative interactions between 1300 protein targets and 6000 ligands. Nucl Acids Res 44: D1054–D1068.

Swensen AM, Herrington J, Bugianesi RM, Dai G, Haedo RJ, Ratliff KS *et al.* (2012). Characterization of the substituted N-triazole oxindole TROX-1, a small-molecule, state-dependent inhibitor of Ca_V2 calcium channels. Mol Pharmacol 81: 488–497.

Timin E, Berjukow S, Hering S (2004). Concepts of state-dependent pharmacology of calcium channels. In: McDonough S (ed). Calcium Channel Pharmacology. Springer: US, pp. 1–19.

Todorovic SM, Meyenburg A, Jevtovic-Todorovic V (2002). Mechanical and thermal antinociception in rats following systemic administration of mibefradil, a T-type calcium channel blocker. Brain Res 951: 336–340.

Tranberg CE, Yang A, Vetter I, McArthur JR, Baell JB, Lewis RJ *et al.* (2012). ω-Conotoxin GVIA mimetics that bind and inhibit neuronal $Ca_V2.2$ ion channels. Mar Drugs 10: 2349–2368.

Tringham E, Powell KL, Cain SM, Kuplast K, Mezeyova J, Weerapura M *et al.* (2012). T-type calcium channel blockers that attenuate thalamic burst firing and suppress absence seizures. Sci Transl Med 4: 121ra19.

Wang F, Yan Z, Liu Z, Wang S, Wu Q, Yu S *et al.* (2016). Molecular basis of toxicity of N-type calcium channel inhibitor MVIIA. Neuropharmacology 101: 137–145.

Waxman SG, Zamponi GW (2014). Regulating excitability of peripheral afferents: emerging ion channel targets. Nat Neurosci 17: 153–163.

Wen XJ, Xu SY, Chen ZX, Yang CX, Liang H, Li H (2010). The roles of T-type calcium channel in the development of neuropathic pain following chronic compression of rat dorsal root ganglia. Pharmacology 85: 295–300.

Wheeler DB, Randall A, Tsien RW (1994). Roles of N-type and Q-type Ca^{2+} channels in supporting hippocampal synaptic transmission. Science 264: 107–111.

Winquist RJ, Pan JQ, Gribkoff VK (2005). Use-dependent blockade of $Ca_V2.2$ voltage-gated calcium channels for neuropathic pain. Biochem Pharmacol 70: 489–499.

Zamponi GW, Feng Z-P, Zhang L, Pajouhesh H, Ding Y, Belardetti F *et al.* (2009). Scaffold-based design and synthesis of potent N-type calcium channel blockers. Bioorg Med Chem Lett 19: 6467–6472.

Zikolova S, Ninov K (1972). Analogs of N^1-benzhydryl-N^4-cinnamylpiperazine (cinnarizine). II. N^1-Substituted-N^4-benzhydrylpiperazines. Tr Nauchnoizsled Khim-Farm Inst 8: 59–67.